ADVANCED MATERIALS
www.advmat.de

A Biodegradable Secondary Battery and its Biodegradation Mechanism for Eco-Friendly Energy-Storage Systems

Myeong Hwan Lee, Jongha Lee, Sung-Kyun Jung, Dayoung Kang, Myung Soo Park, Gi Doo Cha, Kyoung Won Cho, Jun-Hyuk Song, Sehwan Moon, Young Soo Yun, Seok Joo Kim, Young Woon Lim, Dae-Hyeong Kim, and Kisuk Kang**

The production of rechargeable batteries is rapidly expanding, and there are going to be new challenges in the near future about how the potential environmental impact caused by the disposal of the large volume of the used batteries can be minimized. Herein, a novel strategy is proposed to address these concerns by applying biodegradable device technology. An eco-friendly and biodegradable sodium-ion secondary battery (SIB) is developed through extensive material screening followed by the synthesis of biodegradable electrodes and their seamless assembly with an unconventional biodegradable separator, electrolyte, and package. Each battery component decomposes in nature into non-toxic compounds or elements via hydrolysis and/or fungal degradation, with all of the biodegradation products naturally abundant and eco-friendly. Detailed biodegradation mechanisms and toxicity influence of each component on living organisms are determined. In addition, this new SIB delivers performance comparable to that of conventional non-degradable SIBs. The strategy and findings suggest a novel eco-friendly biodegradable paradigm for large-scale rechargeable battery systems.

Rechargeable batteries are indispensable in the new energy paradigm ranging from renewable energy production to electric vehicles and are an important enabler of environmentally benign energy solutions.[1] Significant advances have been made in battery technologies,[2] with a corresponding rapid increase in the mass production of batteries. Even further increases in battery production are expected in the near future to meet the surging demand for electric vehicles and large-scale energy storage systems. Although these changes are beneficial in expediting the shift to a clean-energy-based society, challenges will soon arise regarding the potential environmental issues caused by the disposal of such a large volume of batteries. Most battery components raise critical environmental concerns because of their decomposition times of over 100 years when disposed in nature[3] and the toxic gases and large amount of CO_2 generated when incinerated. Not only the known toxic substances such as cobalt/nickel or fluoride from the cathode and electrolyte but also the non-degradable synthetic materials in the battery can have severe harmful effects on biological systems, including cell death, organ damage, and even the death of living organisms. The impact of these issues would not be negligible and thereby cannot be ignored, particularly as the demand for battery consumption is drastically increasing. Although the recycling of

M. H. Lee, Dr. J. Lee, Dr. S.-K. Jung,[+] D. Kang, G. D. Cha, K. W. Cho, S. Moon, Dr. S. J. Kim, Prof. D.-H. Kim, Prof. K. Kang
Center for Nanoparticle Research
Institute for Basic Science (IBS)
Seoul 08826, Republic of Korea
E-mail: dkim98@snu.ac.kr; matlgen1@snu.ac.kr

M. H. Lee, Dr. S.-K. Jung,[+] J.-H. Song, S. Moon, Prof. D.-H. Kim, Prof. K. Kang
Department of Materials Science and Engineering
Research Institute of Advanced Materials (RIAM)
Seoul National University
Seoul 08826, Republic of Korea

The ORCID identification number(s) for the author(s) of this article can be found under https://doi.org/10.1002/adma.202004902.

[+]Present address: Next Generation Battery Lab, Material Research Center, Samsung Advanced Institute of Technology (SAIT), Samsung Electronics Co., Ltd., 130 Samsung-ro, Yeongtong-gu, Suwon-si, Gyeonggi-do 16678, Republic of Korea

Dr. J. Lee, D. Kang, G. D. Cha, K. W. Cho, Dr. S. J. Kim, Prof. D.-H. Kim, Prof. K. Kang
School of Chemical and Biological Engineering
Institute of Chemical Processes
Seoul National University
Seoul 08826, Republic of Korea

Dr. M. S. Park, Prof. Y. W. Lim
School of Biological Sciences and Institute of Microbiology
Seoul National University
Seoul 08826, Republic of Korea

Prof. Y. S. Yun
KU-KIST Graduate School of Converging Science and Technology
Korea University
145 Anam-ro, Seongbuk-gu, Seoul 02841, Republic of Korea

Prof. K. Kang
Institute of Engineering Research
College of Engineering
Seoul National University
Seoul 08826, Republic of Korea

DOI: 10.1002/adma.202004902

the disposed batteries and/or their toxic elements presents the promising outlook for the sustainability of the rechargeable batteries, many limitations to fulfill the recycling of a large volume of disposed batteries have yet to be overcome, such as the additional cost for the treatment of the disposed batteries and the secondary environmental pollutions from the waste water, the waste gas, and the waste residue during the recycling process.[4] Therefore, alternative approaches are necessary to achieve the significantly improved sustainability and minimize the environmental hazards associated with the continuously increasing amount of the battery production.

Attempts have been made to apply a few biodegradable,[5] bioresorbable,[6] or transient[7] materials as electrodes in the conventional primary battery systems[8] because their relatively fast decomposition can partly reduce the accumulation of overall battery waste.[3] Specifically, electrode chemistries, derived from natural redox-active organics has often been explored, serving as a first step toward the realization of eco-friendly batteries.[9] Although these attempts on the development of the potentially biodegradable batteries were insightful, most of the works up to now have been limited to the development of an individual component (i.e., each of electrode, electrolyte, binder, separator, and package) of the battery system. Some of the transient and partially biodegradable batteries were previously reported,[10] however, such batteries still contain non-biocompatible components. And, it is noted that only a single toxic component can make the overall system harmful to the biological systems. Attempts to make the fully biodegradable battery have been made, however it has been only realized in the primary battery system which could not be recharged.[11] Therefore, the complete demonstration of an eco-friendly rechargeable battery system which is composed of fully biodegradable and non-toxic components has not yet been realized, which is of importance for the next generation sustainable energy storage. Moreover, the quantitative evaluation of the toxicity effect of the disposed batteries are imperative protocols to minimize potentially severe environmental and biological damages of large amounts of disposed batteries in the future. However, the chemical/biological evolution of the commercial battery components and their constituent materials after their disposal has not been studied in depth, still remaining unclear.

Herein, we propose a novel material and device integration strategy for preparing biodegradable Sodium-ion secondary batteies (SIBs). Through extensive screening processes and the testing of a wide selection of candidates, the cathode, anode, binder, separator, electrolyte, and package materials were carefully designed and fabricated (**Table 1**). Among the various cathode candidates, sodium- and iron-based polyanion compounds were determined to be biodegradable and non-toxic. The other battery components were selected by considering their compatibility with the sodium chemistry as well as their biodegradability, including a pyroprotein-based carbon anode, propylene carbonate electrolyte that is known for its high biodegradability,[12] cellulose-based separator, and cellulose/polyester/silicon-based package materials. The detailed biodegradation mechanisms, i.e., hydrolytic and/or fungal biodegradation, were profoundly analyzed for each component, as will be discussed in detail later. Although there are several standard tests and certifications (ASTM, OECD, and ISO) to validate the biodegradability and biocompatibility of a given material under specific environmental conditions,[13] there is currently no standardized test to analyze biodegradation of secondary batteries, according to our knowledge. Therefore, we established a new guideline to verify the biodegradability and the non-toxicity of biodegradable compounds from the secondary batteries via the cytotoxicity test. A cell cytotoxicity assay was used to assess the toxicity influence of the battery materials and their biodegradation products on biological systems. Their macroscopic non-toxicity was also confirmed by the prevalence of microorganisms and the growth of plants. Finally, we demonstrated a biodegradable rechargeable SIB designed using this proposed strategy provided comparable performance to that of conventional SIBs and successfully supplied power to a global positioning system (GPS) in a moving vehicle.

The biodegradable material, in our study, is defined as a material which can completely or partially degrade into simple compounds through the action of microorganisms, such as fungi, bacteria, and algae, with water and oxygen in the natural environment. This definition of the biodegradable material differs from those of the transient and bioresorbable materials; the transient material is capable of disappearing with minimal or non-traceable residues over a period of stable operation, and the bioresorbable material can be broken down and absorbed by body.[14] To screen the biodegradable rechargeable battery materials, the materials were carefully selected by using the following criteria: 1) the candidate materials should be decomposed or degrade naturally within one year, 2) the degradation products from the biodegradable materials should be non-toxic, 3) the materials that are naturally stable and non-toxic, such as the carbon materials, can be candidates, 4) the candidate materials are selected only in the range of materials for the sodium ion battery, because the sodium ion has the lowest toxicity among commonly used cations for battery chemistry. As a result, we could figure out a list of screened candidates as tabulated in Table 1. It was found that the materials colored in green in Table 1 are predicted to be suitable for the components of the biodegradable rechargeable SIB. The materials constituting each component of the proposed biodegradable SIB are schematically shown in **Figure 1**a. $Na_4Fe_3(PO_4)_2(P_2O_7)$ (NFP)[15,16] and pyroprotein-based carbon[17,18] with binders of cellulose derivatives were selected to fabricate the biodegradable composite electrode (cellulose acetate (CA) for the cathode and carboxymethyl cellulose (CMC) for the anode, respectively), and was coated on the aluminum (Al) current collector. The Al current collector, which is not generally biodegradable, was selected, since it could be dissolved after the biodegradation of NFP, which results in the acidic condition (see Figure S5 and Note S1, Supporting Information). A porous CA mesh was used as a separator to prohibit direct contact of the electrodes and provided ion-conducting paths between them. Sodium perchlorate ($NaClO_4$; 1 M) in a propylene carbonate (PC) solution was selected as a biodegradable electrolyte. The electrochemical cell was safely protected from water and oxygen by encapsulation in a biodegradable pouch, a multilayered film of CMC, silicon, and aliphatic copolyester [poly(butylene adipate-*co*-terephthalate); PBAT]. These cathode, anode, binder, current collector, separator, electrolyte, and package materials were demonstrated to exhibit superb biodegradability compared with conventional

Table 1. Biodegradation characteristics of battery component candidates.

Materials	Degradability (Time)	Degradation Pathway	Degradation Products	Ref. (in SI)
Cathode				
$Na_4Fe_3(PO_4)_2(P_2O_7)$	O	H	Na^+, Fe^{2+}, PO_4^{3-}, $P_2O_7^{4-}$	
$NaFePO_4$	X	X	X	
Na_2FePO_4F	O	H	Na^+, Fe^{3+}, PO_4^{3-}, F^-	
$NaFe_{0.5}Mn_{0.5}O_2$	X	X	X	
$NaCoO_2$	X	X	X	
$NaMnO_2$	X	X	X	
$NaFeO_2$	X	X	X	
Anode				
Pyroprotein carbon	☆	–	–	
Graphite	☆	–	–	
Hard carbon	☆	–	–	
Sb	X	–	–	
Ge	X	–	–	
P	X	–	–	
Electrolyte				
$NaClO_4$	O	Oxidation	Na, Cl	#1
PC (Propylene carbonate)	O	M	Propylene glycol, CO_2	#2
DMC (Dimethyl carbonate)	O	M	X	#3
EC (Ethylene carbonate)	X	X	X	
DEC (Diethyl carbonate)	X	X	X	
EMC (Ethylmethyl carbonate)	X	X	X	
glyme (Dimethoxyethane)	X	X	X	
Binder				
Cellulose acetate	O	M	Glucose	#4
Carboxymethyl cellulose	O	M	Glucose	#5
Gelatin derivatives	O	M	Amino acid	#6, #7
Alginate derivatives	O	M	β-D-Mannuronate, α-L-guluronate	#8, #9
PEO (Poly(ethylene oxide))	O	H	PEO	
PVA (Poly(vinyl alcohol))	O	H	PVA	
PTFE	X	X	X	
PVDF	X	X	X	
AB (Acetylene black)	X	X	X	
PAA (Poly(acrylic acid))	X	X	X	
SBR (Styrene-butadiene rubber)	X	X	X	
PVP (Poly(vinylpyrrolidone))	X	X	X	
Separator				
Cellulose acetate	O	M	Glucose	#4
Egg shell membrane	O	H	Amino acid	#10
Nylon series	Δ	H	Amino acid	#11
PEO, PPO	O	H	PEO, PPO	
PE (Polyethylene)	X	M	CO_2	
PP (Polypropylene)	X	M	CO_2	
PVC	X	X	X	
PAN	X	X	X	
PTFE	X	X	X	

Table 1. Continued.

Materials	Degradability (Time)	Degradation Pathway	Degradation Products	Ref. (in SI)
Packaging				
PBAT(Ecoflex)	O	M, H	Lactic acid, adipic acid, 1,4-Butanediol, terephthalic acid	#12
PLA/PLGA	O	M, H	Lactic acid, glycolic acid	#13
Ecovio	O	M, H	Lactic acid, adipic acid, 1,4-Butanediol, terephthalic acid	#12
Nylon (Polyamide)	Δ	H	Diacids, diamine	#11
EVOH (Ethylene vinyl alcohol)	O	H	EVOH	
PE	Δ	M	CO_2	#14
PET	X	X	X	
PAN	X	X	X	
SURLYN	X	X	X	

O: Biodegradable, Δ: Biodegradation time of more than several tens of years, X: Negligible or no biodegradation. ☆: Naturally stable and non-toxic, H: Biodegradation by hydrolysis, M: Biodegradation by microorganisms. Materials colored green in the table are the battery components used for the biodegradable rechargeable SIB in this work.

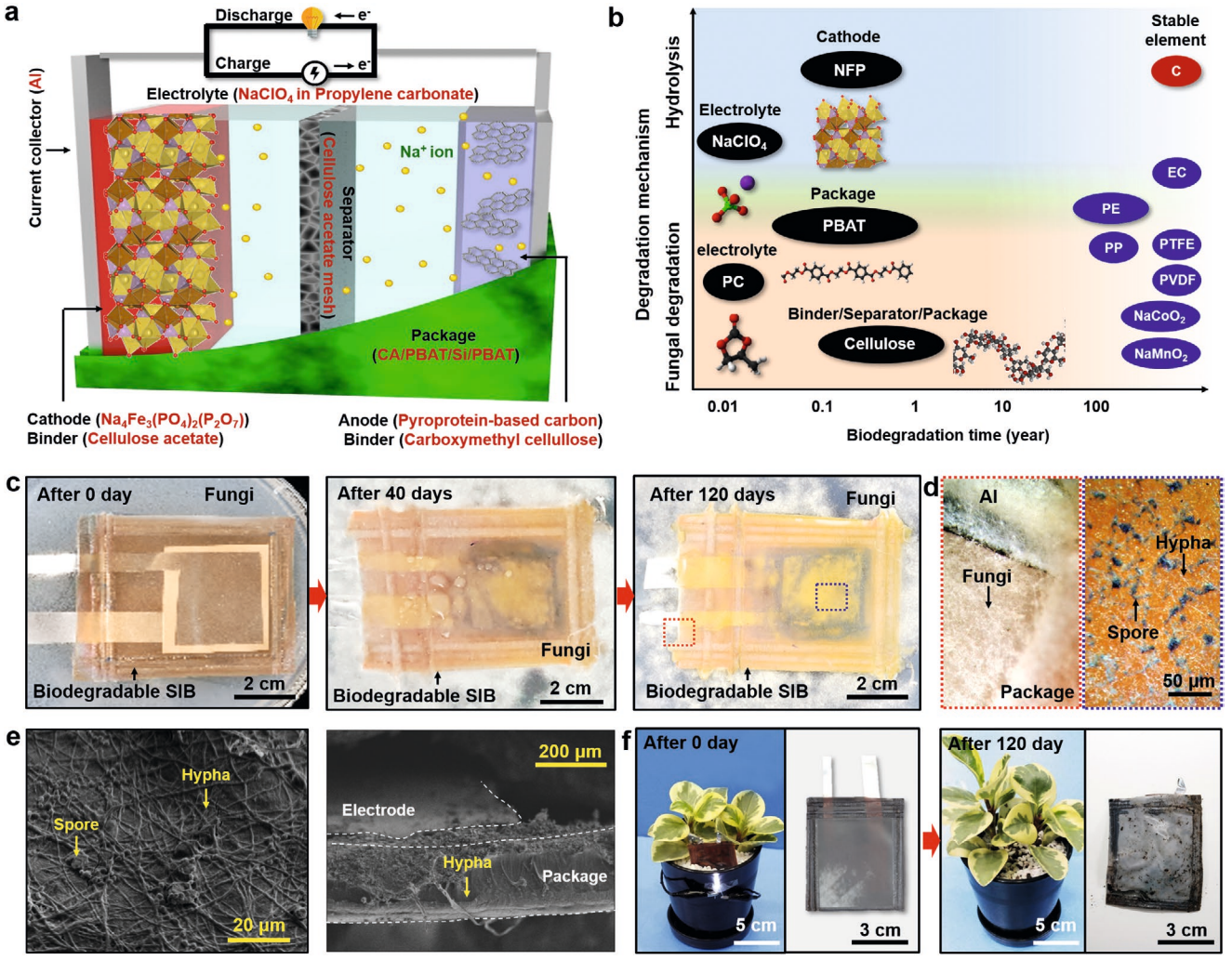

Figure 1. System overview, materials, and biodegradation of the SIB. a) Schematic illustration of the materials and battery structure. b) Biodegradation mechanism after brief biodegradation times for various battery components. c) Image of a biodegradable rechargeable SIB pouch cell after 0, 40, and 120 days of fungal degradation; d) magnified views of boxed areas in (c). e) Top-view and cross-sectional SEM images of biodegradable battery after 120 days of fungal degradation. f) Image of a plant (left side) and buried battery (right frame) on day 0 (left) and day 120 (right) after burial of the SIB in the plant soil.

binders (e.g., poly(tetrafluoroethylene) (PTFE), poly(vinylidene fluoride) (PVDF)), separators (e.g., polyethylene (PE), polypropylene (PP)), and electrolytes (e.g., ethylene carbonate (EC), dimethoxyethane (DME)), as discussed in detail later. NFP and $NaClO_4$[19] dissolve into earth-abundant elemental cations and anions via hydrolysis, whereas other components such as PBAT,[20] cellulose derivatives (CA[21] and CMC[22]), carboxymethyl polyester,[23] PC,[12] and pyroprotein-based carbon are disintegrated through fungal metabolism (Figure 1b).

When the biodegradable sodium-ion battery (SIB) is disposed, the pouch that protects the battery components inside the package will be contacted to water/moisture and microorganisms in the air and soil. The natural degradation of the biodegradable pouches will be initiated at the surface, where the package is exposed to the fungi in the soil. The degradation will propagate into the inside of the pouch, reach the internal components at some point, and initiate the biodegradation of the internal components. The tetralayered pouch dissociates into silicic acid, glucose, terephthalate, adipate, and 1,4-butanediol after the natural microbial degradation reactions (cellulose) and the hydrolysis reactions (Si and PBAT). When the pouch can no longer protect the battery components inside the pouch due to its biodegradation, the water/moisture and microorganisms will penetrate into the package and be contacted to the battery components inside the pouch, triggering the natural degradation of internal components via hydrolysis and/or fungal degradation reactions. As discussed in the next section in more detail, the cathode is hydrolyzed into sodium, iron, phosphate, and pyrophosphate; and the binder is transformed into glucose after its biodegradation. The cellulose mesh separator is transformed into glucose[24] via the fungal degradation. The electrolyte is decomposed via various mechanisms, of which the representative products include ethanol, methanol, carbon dioxide, propylene glycol,[12] sodium, and chloride[19] via natural hydrolysis (PC) and microbial degradation (sodium perchlorate), as shown Figure 1b and Figure S1 (Supporting Information). Thus, none of the components of the SIB produces toxic substances or non-degradable wastes after biodegradation. The non-toxicity of the SIB was confirmed using living organisms. As shown in Figure 1c–e, the degraded SIB did not adversely affect the growth of microorganisms such as Basidiomycota and Ascomycota. The growth of larger organisms such as a plant (peperomia) was also not affected, as shown in Figure 1f.

Among electrode material candidates, sodium/iron-based materials have been intensively investigated because of their elemental non-toxicity.[25] We synthesized various sodium/iron-based cathode materials, the structures of which were based on either phosphate–polyanion frameworks ($Na_4Fe_3(PO_4)_2(P_2O_7)$, $NaFePO_4$, and Na_2FePO_4F) or oxides ($NaFe_{0.5}Mn_{0.5}O_2$, $NaCoO_2$, $NaMnO_2$, and $NaFeO_2$). X-ray diffraction patterns of each sample are presented in Figure S2 (Supporting Information).[26] We studied their degradation mechanisms, starting with their hydrolysis (**Figure 2**a). The cathode materials were placed in water with continuous stirring for 3 days, and the concentration of solubilized ions was measured using inductively coupled plasma-atomic emission spectroscopy (ICP-AES). The transition metal ions in the crystal structure, together with sodium ions, were dissolved in the water together in case of the polyanion compounds (Figure 2a, left). In contrast, only sodium was hydrolyzed in case of the layered oxides (Figure 2a, right) even under acidic conditions (pH 2; Figure S3, Supporting Information). These differences resulted in morphological changes only in the polyanions. The detailed morphological change of the representative polyanion material, NFP, was examined using scanning electron microscopy (SEM). NFP became more porous because of the dissolution of the main crystal framework (Figure 2b). Another polyanion material, Na_2FePO_4F, showed similar morphological changes (Figure S4a, Supporting Information). On the other hand, the morphologies of the layered oxides, such as $NaMnO_2$ and $NaFeO_2$, remained intact (Figure S4b,c, Supporting Information). It is widely known that the intact morphologies of the layered oxides in water are induced from both the H^+/H_2O intercalation into the layered structure and the negligible dissolution of the transition metal ions.[27] Among the sodium/iron-based cathode materials, NFP was selected as a cathode material because of its rapid hydrolysis during biodegradation (Figure 2c). The hydrolyzed products of NFP could be speculated using the Pourbaix diagram with the atomic ratio of NFP (Na:Fe:P = 4:3:4) (Figure 2d).[28] Under the conditions observed in natural soil (Figure 2d, green box),[29] NFP tends to be solubilized into elemental (Na^+ and Fe^{2+}) and polyatomic ($H_2PO_4^-$ and HPO_4^{2-}) ions. In particular, the complete dissolution of NFP is preferably preceded when the pH is slightly lower than ≈7.

The anode, binder, separator, electrolyte, and package also undergo hydrolysis; however, their decomposition rates were greatly accelerated by fungal biodegradation. To investigate the detailed kinetics of their fungal biodegradation, each battery component was inoculated with a mixture of representative fungi (e.g., *Aspergillus niger*, *Aureobasidium pullulans* var. *pullulans*, *Chaetomium globosum*, *Penicillium bialowiezense*, *Talaromyces pinophilum*, and *Trichoderma virens*). Figure 2e–h present SEM images (top view) of the battery components, and Figure 2i presents an SEM image of the dried hydrogel composed of agar, water, and the 3% v/v electrolyte after 40 days of fungal inoculation. The SEM images reveal the satisfactory growth of the inoculated fungi on all the battery components. *Trichoderma virens* (Figure S6, Supporting Information) colonized well on the surface of the cathode, anode, and package (SEM images in Figure 2e–g; corresponding optical images in Figure S7a–c, Supporting Information). In addition, the hyphae of *Talaromyces pinophilum* adhered well to the anode, package, and separator and even penetrated into the package (Figure 2f–h; corresponding optical images in Figure S7b–d, Supporting Information). Both species grew particularly well in the presence of the electrolyte (Figure 2i and Figure S6, Supporting Information) and in the pure polymer (Figure S8, Supporting Information). Furthermore, these results confirm that the fungi utilized the battery components as resources for their colonization.[3] Because of the fungal metabolism, a mass decrease of the battery components was observed after 120 days of inoculation (Figure 2j–n; complete biodegradation in Figure 2n results in the concentration under the limit of detection (0.005 wt%)). Although the complete biodegradation of the components will require more time in most cases, the weight decrease due to the biodegradation signifies the use of these materials as nutrients for the growth of fungi.

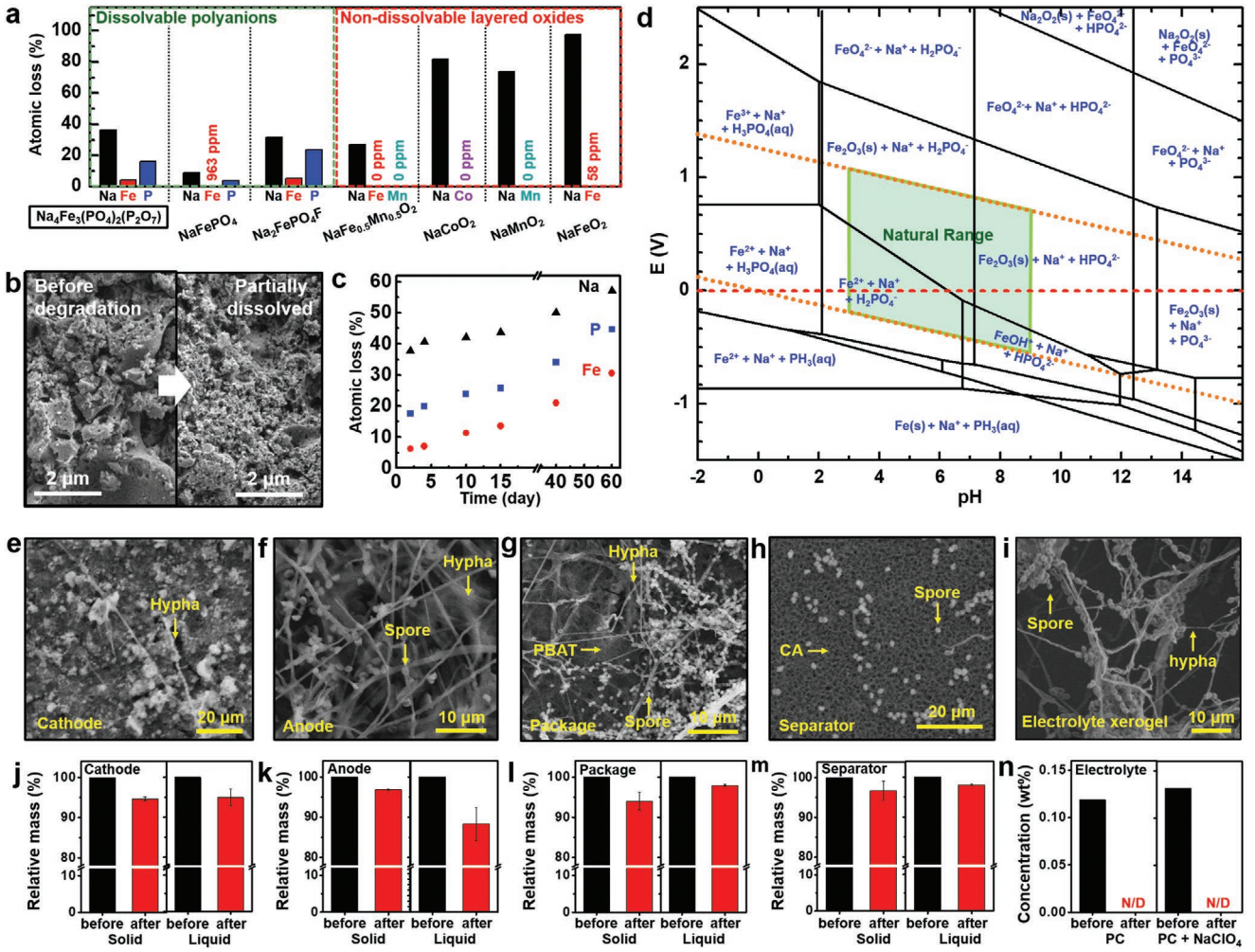

Figure 2. Hydrolytic and fungal biodegradation of battery components. a) Concentration of solubilized metal ions originated from various sodium- and iron-based cathode materials after 3 days of hydrolysis. b) SEM image of NFP before (left) and after (right) 60 days of hydrolysis. c) Plot of solubilized ions (% of the mass loss) of NFP as a function of time. d) Pourbaix diagram of sodium, iron, and phosphorous, which has been adopted from Materials Project (www.materialsproject.org), whose detailed calculation methods are provided in ref. [28]. The energy and pH ranges found in nature are indicated by the green region. e–i) SEM images of the: e) cathode, f) anode, g) package, h) separator, and i) dried 3% v/v electrolyte hydrogel after fungi inoculation. The images were captured after 40 days of inoculation and freeze-drying. j–m) Mass loss of the: j) cathode, k) anode, l) package, and m) separator (% of the initial mass) in the solid medium (left) and liquid medium (right). n) Mass loss of electrolyte (wt%) without (left) and with (right) $NaClO_4$ after 120 days of inoculation (N/D stands for non-detected).

The battery components and their degradation products may have adverse effects on the biology of living organisms such as individual cells and/or microorganisms. For example, cobalt, which is a widely used element for cathode materials, can induce the complete or partial death of cells at concentrations of 1×10^{-3} M or less (**Figure 3**a). Therefore, the effect of each battery material on the cell viability was systemically tested to evaluate the safety and toxicity. We used human umbilical vein endothelial cells (HUVECs) for the cytotoxicity test because of their known sensitivity to the culture environment.[30] The toxicity was investigated using the tetrazolium-based colorimetric assay (MTT assay; Figure 3b). The cathode, anode, separator, and package were individually placed in the cell medium or deionized water under vigorous stirring for 3 days, and the extracts were sterilized and used for the MTT assay. None of the SIB component materials exhibited any significant toxicity, and some components (NFP, CA as a representative cellulose, and carbon) unexpectedly promoted the growth of the HUVECs because materials in the extracts (e.g., glucose, phosphate, and iron) acted as nutrients for the cell metabolism.[31]

The non-toxicity of the degradation products was subsequently investigated. After the complete dissolution of the cathode, it was hydrolyzed into Na^+, Fe^{2+}, $H_2PO_4^-$, and HPO_4^{2-}. Because the biological toxicity of some metal ions is already known,[32,33] we established a toxicity spectrum of representative metal ions that are commonly used for the electrodes using the MTT assay of the HUVECs. We identified the characteristic toxic concentration (CC50) of the target ion of the degradation products, the concentration which leads to the cell death of 50% by systematically varying the concentration

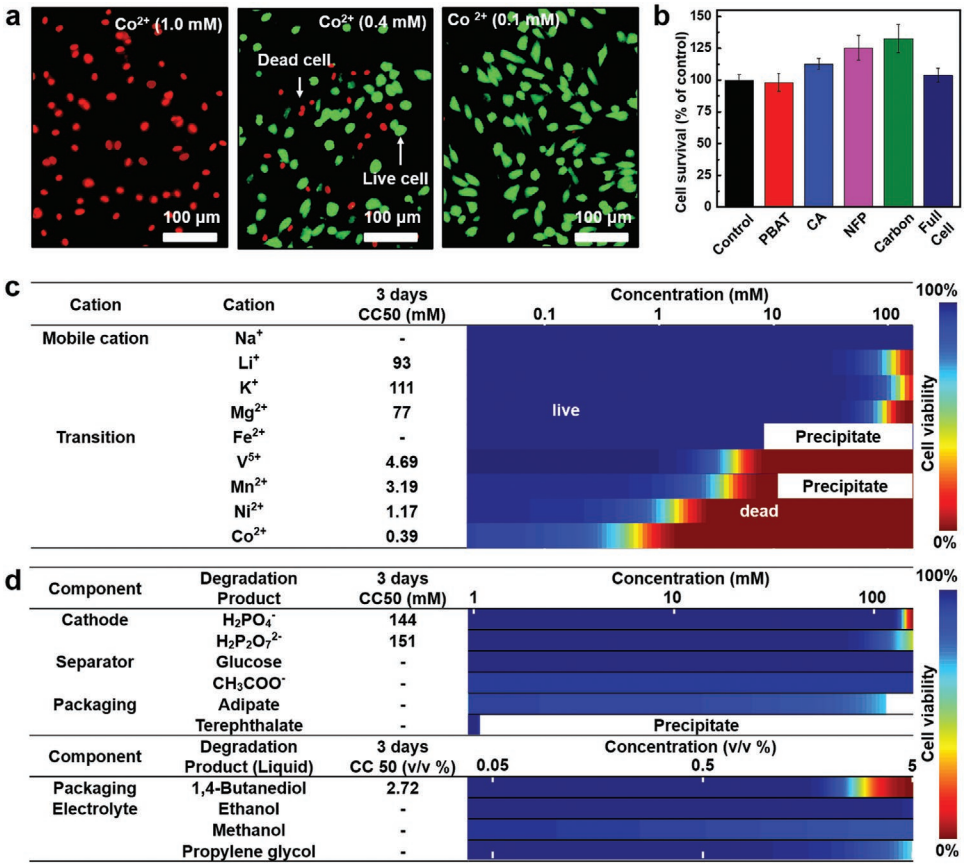

Figure 3. Material safety and toxicity of battery components and biodegradation products. a) Live and dead cell viability assay with 1.0×10^{-3} M (left), 0.4×10^{-3} M (middle), and 0.1×10^{-3} M (right) Co^{2+} in the cell culture medium. b) MTT cell viability assay of each battery component. c) MTT cell viability assay result as a function of the concentration of various metal ions, and calculated CC50 of various metal ions. d) MTT cell viability assay result as a function of the ion concentration while varying the concentration of the degraded products from the battery components, and calculated CC50 of various degradation products of the battery components.

of the target ion in the cell medium, as shown in Figure 3c,d. Sodium induced no cell death even at 160×10^{-3} M, and iron did not exhibit any toxicity up to its maximum soluble concentration (8×10^{-3} M in the cell medium). As a reference, magnesium, lithium, and potassium exhibited a CC50 of $\approx 100 \times 10^{-3}$ M. The high CC50 values of sodium and iron confirms their biological safety, whereas the low CC50 values of nickel and cobalt indicate their toxicity[32] to the cells. A similar toxicity spectrum was obtained for the anions. The anionic degradation products of NFP (cathode), i.e., dihydrogen phosphate and dihydrogen pyrophosphate ions, exhibited a CC50 of $\approx 100 \times 10^{-3}$ M, confirming their biological safety (Figure 3d). After the fungal and hydrolytic degradation of the other battery components, glucose (from the binder and separator); terephthalate and 1,4-butanediol (from the package); and ethanol, methanol, and propylene glycol (from the electrolyte) were produced. All these degradation products exhibited high CC50 values, confirming their material non-toxicity (Figure 3d).[34] Carbon is an insoluble non-toxic degradation product of the anode (Figure 3b), which is widely found in nature.[35] Notably, neither the components nor their biodegradation products disturbed the growth of the HUVECs, and some even promoted cell growth.

We evaluated the electrochemical performance of the NFP cathode and pyroprotein-based carbon anode with the cellulose derivative binder in a half cell before fabricating the full cell. The NFP cathode exhibited a voltage profile similar to that previously reported[15,16] with a specific charge–discharge capacity of ≈110 mAh g^{-1} (**Figure 4**a). The NFP cathode fabricated using cellulose-based biodegradable binders exhibited comparable performance to that using commercial binders (e.g., PVDF), confirming cycling stability (Figure 4b). The cycle retention of the NFP electrode with the biodegradable binder reached ≈93% after 100 cycles at a current rate of 20 mA g^{-1}, which is a higher retention than that with PVDF (≈89%). The charge–discharge profile of the negative electrode (pyroprotein-based carbon) is presented in Figure 4c, indicating that a capacity of 190 mAh g^{-1} was stably maintained during 50 cycles (Figure 4d).

The electrochemical stability, electrolyte wettability, and pore size of the CA mesh used as a biodegradable battery separator were also examined. The electrochemical stability of the cellulose (CA) mesh separator was tested using Na plating/stripping cycles with a Na/Na symmetric cell. In Figure 4e, the plating/stripping cycle profiles of the CA mesh are compared with those of a glass fiber filter (GFF) and commercialized Celgard separator with a current density of 1 mA cm^{-2} after a 1 h

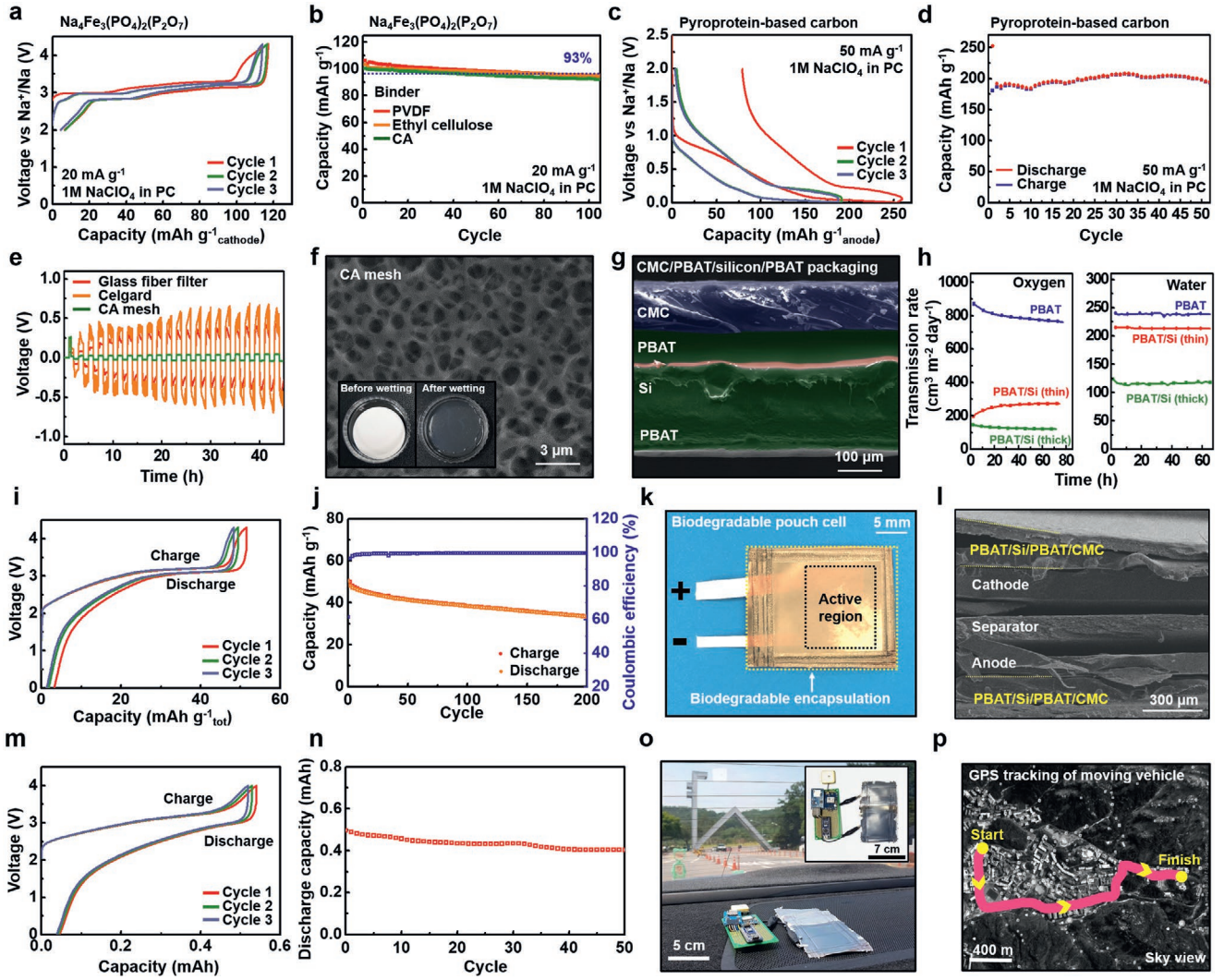

Figure 4. Electrochemical performance and system demonstration of the SIB. a) Charge–discharge profiles of NFP in the Na half-cell. b) Cyclic stability of NFP with the CA binder. c) Charge–discharge profiles of the pyroprotein-based carbon electrode in the Na half-cell. d) Cyclic stability of the pyroprotein-based carbon anode with the CMC binder. e) Galvanostatic cycling performance of Na/Na symmetric cells with a current rate of 1 mA cm^{-2}. f) Magnified SEM image of the CA mesh separator. The inset presents photographs of the CA mesh before (left) and after (right) wetting with PC. g) Cross-sectional SEM image of the package (100 μm CMC, 70 μm PBAT, 10 μm Si, and 200 μm PBAT). h) Oxygen (left) and water vapor (right) transmission rate with (red, green) and without (blue) the silicon interlayer. i) Charge–discharge profiles of the fabricated coin cell at 20 mA g^{-1}. j) Cycling performance of the coin cell at 50 mAh g^{-1} in the 0.1–4.15 V range. k) Photograph and l) cross-sectional SEM image of the fabricated pouch cell. m) Charge–discharge profiles of the pouch cell at a current rate of 0.15 mA cm^{-2}. n) Cycling performance of the single-layer pouch cell. o) Photograph of the system during tracking of the position of a moving vehicle. The inset presents a photograph of the custom-made GPS. p) Position tracking of a moving vehicle using the GPS powered by the biodegradable SIB.

rest. Interestingly, the CA mesh separator showed consistently lower hysteresis of plating and stripping voltages than those for the GFF and Celgard separator, indicating a low resistance of the CA mesh separator. This low resistance was attributed to the good wettability of the CA mesh separator to the electrolyte, as shown in the inset of Figure 4f. Together with the uniform pore size distributions (≈2 μm) shown in Figure 4f, the good wettability aided in the enhancement of the electrochemical kinetics in the cell, as shown in Figure 4e.

We also developed a CMC/PBAT/Si/PBAT multilayered package to encapsulate all the battery components and protect them from moisture and oxygen (Figure 4g). For the package fabrication, a silicon thin film was deposited on the CMC/PBAT film by radio-frequency sputtering, and the exposed silicon layer was coated again with a PBAT film. The developed package exhibited good waterproof and airproof properties (Figure 4h), as the multilayer structure with the 10 μm interlayer silicon film dramatically suppressed water and oxygen permeation. The water permeability could be further suppressed by adding a thick magnesium foil (Figure S9a, Supporting Information). Furthermore, the foldable property and the curvature of the biodegradable pouch, composed of a multilayer of CMC/PBAT/Si/PBAT coated on the magnesium metal foil, are similar with the commercial aluminum pouch as shown in Figure S10

(Supporting Information), confirming its mechanical feasibility as reliable packaging material.

Before we assembled each battery component in the CMC/PBAT/Si/PBAT multilayered package, we first constructed a coin cell using the NFP cathode, pyroprotein-based carbon anode, CA mesh separator, and $NaClO_4$/PC electrolyte to evaluate the full cell performance (see Note S2 (Supporting Information) for electrochemical reactions of the full cell). The coin cell exhibited a discharge voltage plateau at ≈3 V with a specific capacity of ≈50 mAh g^{-1} based on the total electrode mass (Figure 4i). Given the specific capacity of NFP and pyroprotein-based carbon, the NP ratio (negative-to-positive electrode mass ratio) was set to be ≈1:2.5.[36] The charge–discharge cyclic experiment confirmed the stable operation of the biodegradable SIB with only a slight decrease of the capacity during 200 cycles (Figure 4j). After characterization of each battery component and confirmation of the half-cell and full-cell performances, we assembled the components in a CMC/PBAT/Si/PBAT multilayered package to construct a biodegradable cell (Figure 4k). We stacked the bottom package, cathode, separator, anode, and top package in series (cross-sectional view in Figure 4l). Similar to the coin cell, the pouch-type biodegradable cell exhibited a discharge voltage plateau near ≈3 V (Figure 4m). For the single-layered pouch cell, the reversible areal charge/discharge capacity of ≈0.12 mAh cm^{-2} could be maintained over 50 cycles (Figure 4n); the capacity of the overall system could be increased by using multiple pouch cells. Additionally, the protective property of the pouch cell was slightly improved by using a magnesium foil package (Figure S9b,c, Supporting Information). The capacity retention of ≈80% after 50 cycles was comparable to that of the reference pouch cell, which is attributed to the effective suppression in the permeation of water and oxygen (Figure S9a, Supporting Information).

The biodegradable SIB cell was then tested by powering a custom-made GPS to track the position of a moving vehicle (Figure 4o). The GPS was composed of the GPS communication unit, a microprocessor, and a memory device (circuit diagram in Figure S11 (Supporting Information), corresponding image in the inset of Figure 4o), with a required voltage of ≈5 V. Three biodegradable SIBs, connected in series, could successfully supply the required power to the system. Using the power supply, the system successfully monitored the position of a moving vehicle (sky view of the entire track in Figure 4p). In addition, the SIB could be recharged repetitively to prolong the monitoring time.

We presented a novel material and device strategy toward the realization of a biodegradable eco-friendly and rechargeable SIB, which can significantly reduce the potential environmental and biological impacts by the disposal of a large volume of used batteries. We selected and/or synthesized high-performance biodegradable materials for the battery components, and their biodegradation kinetics were systematically and extensively studied. All the components of the biodegradable SIB developed here can be naturally disintegrated via hydrolysis and/or fungal biodegradation. The material non-toxicity and environmental benignity of the battery components and degradation products were confirmed by cell cytotoxicity tests. The assembled full cell exhibited reasonable electrochemical performance compared with that of conventional non-degradable SIBs. Once this biodegradable battery and the related analysis methods are certified by the standardized tests from ASTM, OECD, and ISO, this biodegradable rechargeable SIB and its validation method will offer a novel paradigm toward the realization of next-generation environmentally benign large-scale rechargeable battery systems while simultaneously contributing to the sustainability of both human lifestyle and nature.

Supporting Information

Supporting Information is available from the Wiley Online Library or from the author.

Acknowledgements

M.H.L., J.L., S.-K.J., and D.K. contributed equally to this work. This work was supported by project code (IBS-R006-A1 and IBS-R006-A2). This work was also supported by the National Research Foundation of Korea (NRF) grants NRF-2019M3E6A1064522, No. 2018R1A2A1A05079249, and by Creative Materials Discovery Program (NRF-2017M3D1A1039553).

Conflict of Interest

The authors declare no conflict of interest.

Keywords

biodegradable batteries, eco-friendly materials, non-toxic materials, sodium-ion rechargeable batteries

Received: July 18, 2020
Revised: December 10, 2020
Published online:

[1] a) D. Lin, Y. Liu, Y. Cui, *Nat. Nanotechnol.* **2017**, *12*, 194; b) Y. Liu, G. Zhou, K. Liu, Y. Cui, *Acc. Chem. Res.* **2017**, *50*, 2895.
[2] a) B. Dunn, H. Kamath, J.-M. Tarascon, *Science* **2011**, *334*, 928; b) C. P. Grey, J. M. Tarascon, *Nat. Mater.* **2017**, *16*, 45; c) L. Gaines, *Sustainable Mater. Technol.* **2014**, *1–2*, 2.
[3] N. Ojha, N. Pradhan, S. Singh, A. Barla, A. Shrivastava, P. Khatua, V. Rai, S. Bose, *Sci. Rep.* **2017**, *7*, 39515.
[4] a) L. J. Fewtrell, A. Prüss-Üstün, P. Landrigan, J. L. Ayuso-Mateos, *Environ. Res.* **2004**, *94*, 120; b) G. WHO, Switzerland, World Health Organization (WHO) **2010**; c) G. WHO, Switzerland, World Health Organization (WHO) **2017**; d) G. Harper, R. Sommerville, E. Kendrick, L. Driscoll, P. Slater, R. Stolkin, A. Walton, P. Christensen, O. Heidrich, S. Lambert, A. Abbott, K. Ryder, L. Gaines, P. Anderson, *Nature* **2019**, *575*, 75; e) E. Fan, L. Li, Z. Wang, J. Lin, Y. Huang, Y. Yao, R. Chen, F. Wu, *Chem. Rev.* **2020**, *120*, 7020; f) L. Zajac, R. W. Kobrosly, B. Ericson, J. Caravanos, P. J. Landrigan, A. M. Riederer, *Environ. Res.* **2020**, *183*, 109251.
[5] a) H. Tao, S.-W. Hwang, B. Marelli, B. An, J. E. Moreau, M. Yang, M. A. Brenckle, S. Kim, D. L. Kaplan, J. A. Rogers, F. G. Omenetto, *Proc. Natl. Acad. Sci. USA* **2014**, *111*, 17385; b) D. Son, J. Lee, D. J. Lee, R. Ghaffari, S. Yun, S. J. Kim, J. E. Lee, H. R. Cho, S. Yoon, S. Yang,

S. Lee, S. Qiao, D. Ling, S. Shin, J.-K. Song, J. Kim, T. Kim, H. Lee, J. Kim, M. Soh, N. Lee, C. S. Hwang, S. Nam, N. Lu, T. Hyeon, S. H. Choi, D.-H. Kim, *ACS Nano* **2015**, *9*, 5937; c) C. M. Boutry, A. Nguyen, Q. O. Lawal, A. Chortos, S. Rondeau-Gagné, Z. Bao, *Adv. Mater.* **2015**, *27*, 6954; d) S.-K. Kang, R. K. J. Murphy, S.-W. Hwang, S. M. Lee, D. V. Harburg, N. A. Krueger, J. Shin, P. Gamble, H. Cheng, S. Yu, Z. Liu, J. G. McCall, M. Stephen, H. Ying, J. Kim, G. Park, R. C. Webb, C. H. Lee, S. Chung, D. S. Wie, A. D. Gujar, B. Vemulapalli, A. H. Kim, K.-M. Lee, J. Cheng, Y. Huang, S. H. Lee, P. V. Braun, W. Z. Ray, J. A. Rogers, *Nature* **2016**, *530*, 71.

[6] a) M. Tsang, A. Armutlulu, A. W. Martinez, S. A. B. Allen, M. G. Allen, *Microsyst. Nanoeng.* **2015**, *1*, 15024; b) X. Huang, D. Wang, Z. Yuan, W. Xie, Y. Wu, R. Li, Y. Zhao, D. Luo, L. Cen, B. Chen, H. Wu, H. Xu, X. Sheng, M. Zhang, L. Zhao, L. Yin, *Small* **2018**, *14*, 1800994.

[7] a) S.-W. Hwang, H. Tao, D.-H. Kim, H. Cheng, J.-K. Song, E. Rill, M. A. Brenckle, B. Panilaitis, S. M. Won, Y.-S. Kim, Y. M. Song, K. J. Yu, A. Ameen, R. Li, Y. Su, M. Yang, D. L. Kaplan, M. R. Zakin, M. J. Slepian, Y. Huang, F. G. Omenetto, J. A. Rogers, *Science* **2012**, *337*, 1640; b) T. Lei, M. Guan, J. Liu, H.-C. Lin, R. Pfattner, L. Shaw, A. F. McGuire, T.-C. Huang, L. Shao, K.-T. Cheng, J. B. H. Tok, Z. Bao, *Proc. Natl. Acad. Sci. USA* **2017**, *114*, 5107; c) J. Lee, B. Yoo, H. Lee, G. D. Cha, H.-S. Lee, Y. Cho, S. Y. Kim, H. Seo, W. Lee, D. Son, M. Kang, H. M. Kim, Y. I. Park, T. Hyeon, D.-H. Kim, *Adv. Mater.* **2017**, *29*, 1603169.

[8] a) T. Sun, Z.-j. Li, H.-g. Wang, D. Bao, F.-l. Meng, X.-b. Zhang, *Angew. Chem., Int. Ed.* **2016**, *55*, 10662; b) Y. J. Kim, W. Wu, S.-E. Chun, J. F. Whitacre, C. J. Bettinger, *Proc. Natl. Acad. Sci. USA* **2013**, *110*, 20912; c) P. Hu, H. Wang, Y. Yang, J. Yang, J. Lin, L. Guo, *Adv. Mater.* **2016**, *28*, 3486; d) K. Fu, Z. Wang, C. Yan, Z. Liu, Y. Yao, J. Dai, E. Hitz, Y. Wang, W. Luo, Y. Chen, M. Kim, L. Hu, *Adv. Energy Mater.* **2016**, *6*, 1502496; e) L. Yin, X. Huang, H. Xu, Y. Zhang, J. Lam, J. Cheng, J. A. Rogers, *Adv. Mater.* **2014**, *26*, 3879.

[9] a) M. Lee, J. Hong, D.-H. Seo, D. H. Nam, K. T. Nam, K. Kang, C. B. Park, *Angew. Chem., Int. Ed.* **2013**, *52*, 8322; b) J. Hong, M. Lee, B. Lee, D.-H. Seo, C. B. Park, K. Kang, *Nat. Commun.* **2014**, *5*, 5335; c) B. Lee, Y. Ko, G. Kwon, S. Lee, K. Ku, J. Kim, K. Kang, *Joule* **2018**, *2*, 61.

[10] a) V. Michel, D. Yoshiharu, H. Karl-Heinz, H. Michael, H. Philip, K. Przemyslaw, R. Marguerite, S. François, *Pure Appl. Chem.* **2012**, *84*, 377; b) Z. Zhu, T. Kin Tam, F. Sun, C. You, Y. H. Percival Zhang, *Nat. Commun.* **2014**, *5*, 3026; c) K. Fu, Z. Liu, Y. Yao, Z. Wang, B. Zhao, W. Luo, J. Dai, S. D. Lacey, L. Zhou, F. Shen, M. Kim, L. Swafford, L. Sengupta, L. Hu, *Nano Lett.* **2015**, *15*, 4664; d) B. J. Kim, D. H. Kim, S. L. Kwon, S. Y. Park, Z. Li, K. Zhu, H. S. Jung, *Nat. Commun.* **2016**, *7*, 11735; e) M. Mohammadifar, I. Yazgan, J. Zhang, V. Kariuki, O. A. Sadik, S. Choi, *Adv. Sustainable Syst.* **2018**, *2*, 1800041.

[11] J. P. Esquivel, P. Alday, O. A. Ibrahim, B. Fernández, E. Kjeang, N. Sabaté, *Adv. Energy Mater.* **2017**, *7*, 1700275.

[12] a) European Chemicals Agency (ECHA; agency of the European Union) https://www.echa.europa.eu/es/web/guest/registration-dossier/-/registered-dossier/16088/5/3/2 (accessed: March 2020); b) *J. Am. Coll. Toxicol.* **1987**, *6*, 23; c) Research Triangle Institute, and Science Applications International Corporation, *Environmental Profile for Propylene Carbonate*, U.S. Environmental Protection Agency, Washington, D.C. **1998**, https://cfpub.epa.gov/si/si_public_record_Report.cfm?Lab=NRMRL&dirEntryID=99479 (accessed: March 2020); d) H.-J. Buysch, *Carbonic Esters: Ullmann's Encyclopedia of Industrial Chemistry*, Wiley, New York **2000**; e) S. Hammes-Schiffer, S. J. Benkovic, *Annu. Rev. Biochem.* **2006**, *75*, 519; f) Propylene Carbonate in Cleaning and Degreasing Applications, https://www.jrhessco.com/propylene-carbonate-in-cleaning-degreasing-applications/ (accessed: March 2020); g) M. F. A. Schmidt, D. Schleheck, B. Schink, N. Müller, *PLoS One* **2014**, *9*, 115902; h) I. Barnes, P. Wiesen, M. Gallus, *RSC Adv.* **2016**, *6*, 98234; i) Y. M. Delavoux, M. Gilmore, M. P. Atkins, M. Swadźba-Kwaśny, J. D. Holbrey, *Phys. Chem. Chem. Phys.* **2017**, *19*, 2867; j) S. Paul, J. Deka, A. Deka, N. K. Gour, *Atmos. Environ.* **2019**, *216*, 116952.

[13] a) OECD, *Test No. 311: Anaerobic Biodegradability of Organic Compounds in Digested Sludge: by Measurement of Gas Production* **2006**, https://www.oecd-ilibrary.org/environment/test-no-311-anaerobic-biodegradability-of-organic-compounds-in-digested-sludge-by-measurement-of-gas-production_9789264016842-en (accessed: March 2020); b) European Bioplastics, e.V., *Certification Scheme Products made of Compostable Materials According to EN13432 if applicable, in connection with ASTM D 6400, EN 14995, ISO17088, ISO18606*, **2016**, https://docs.european-bioplastics.org/publications/EUBP_Seedling_Certification_Scheme_2020.pdf (accessed: January 2021).

[14] A. Zvezdin, E. Di Mauro, D. Rho, C. Santato, M. Khalil, *MRS Energy Sustainability* **2020**, *7*, E16.

[15] a) H. Kim, I. Park, D.-H. Seo, S. Lee, S.-W. Kim, W. J. Kwon, Y.-U. Park, C. S. Kim, S. Jeon, K. Kang, *J. Am. Chem. Soc.* **2012**, *134*, 10369; b) H. Kim, I. Park, S. Lee, H. Kim, K.-Y. Park, Y.-U. Park, H. Kim, J. Kim, H.-D. Lim, W.-S. Yoon, K. Kang, *Chem. Mater.* **2013**, *25*, 3614; c) M. H. Lee, S. J. Kim, D. Chang, J. Kim, S. Moon, K. Oh, K.-Y. Park, W. M. Seong, H. Park, G. Kwon, B. Lee, K. Kang, *Mater. Today* **2019**, *29*, 26.

[16] a) X. Wu, G. Zhong, Y. Yang, *J. Power Sources* **2016**, *327*, 666; b) A. J. Fernández-Ropero, M. Zarrabeitia, M. Reynaud, T. Rojo, M. Casas-Cabanas, *J. Phys. Chem. C* **2018**, *122*, 133; c) X. Ma, X. Wu, P. Shen, *ACS Appl. Energy Mater.* **2018**, *1*, 6268.

[17] a) S. Y. Cho, Y. S. Yun, S. Lee, D. Jang, K.-Y. Park, J. K. Kim, B. H. Kim, K. Kang, D. L. Kaplan, H.-J. Jin, *Nat. Commun.* **2015**, *6*, 7145; b) S. Y. Cho, Y. S. Yun, D. Jang, J. W. Jeon, B. H. Kim, S. Lee, H.-J. Jin, *Nat. Commun.* **2017**, *8*, 74.

[18] a) P. Liu, Y. Li, Y.-S. Hu, H. Li, L. Chen, X. Huang, *J. Mater. Chem. A* **2016**, *4*, 13046; b) L. Wu, D. Buchholz, C. Vaalma, G. A. Giffin, S. Passerini, *ChemElectroChem* **2016**, *3*, 292; c) T. Zhang, J. Mao, X. Liu, M. Xuan, K. Bi, X. L. Zhang, J. Hu, J. Fan, S. Chen, G. Shao, *RSC Adv.* **2017**, *7*, 41504; d) A. Raj K, M. R. Panda, D. P. Dutta, S. Mitra, *Carbon* **2019**, *143*, 402.

[19] J. Xu, Y. Song, B. Min, L. Steinberg, B. E. Logan, *Environ. Eng. Sci.* **2003**, *20*, 405.

[20] K. Fukushima, A. Rasyida, M.-C. Yang, *Appl. Clay Sci.* **2013**, *80–81*, 291.

[21] M. R. Calil, F. Gaboardi, C. G. F. Guedes, D. S. Rosa, *Polym. Test.* **2006**, *25*, 597.

[22] B. B. Anita, A. J. Thatheyus, D. Ramya, *Sci. Int.* **2013**, *1*, 85.

[23] M. Yamamoto, U. Witt, G. Skupin, D. Beimborn, R.-J. Müller, in *Biopolymers Online: Biology Chemistry Biotechnology Applications*, John Wiley & Sons, Inc., Hoboken, NJ, USA **2005**.

[24] L. E. R. Berghem, L. G. Pettersson, *Eur. J. Biochem.* **1973**, *37*, 21.

[25] R. D. McKerracher, C. Ponce de Leon, R. G. A. Wills, A. A. Shah, F. C. Walsh, *ChemPlusChem* **2015**, *80*, 323.

[26] M. Avdeev, Z. Mohamed, C. D. Ling, J. Lu, M. Tamaru, A. Yamada, P. Barpanda, *Inorg. Chem.* **2013**, *52*, 8685.

[27] a) M. Butel, L. Gautier, C. Delmas, *Solid State Ionics* **1999**, *122*, 271; b) H. Kim, J. Hong, K.-Y. Park, H. Kim, S.-W. Kim, K. Kang, *Chem. Rev.* **2014**, *114*, 11788; c) A. Ramanujapuram, D. Gordon, A. Magasinski, B. Ward, N. Nitta, C. Huang, G. Yushin, *Energy Environ. Sci.* **2016**, *9*, 1841; d) Y. Cho, M. H. Lee, H. Kim, K. Ku, G. Yoon, S.-K. Jung, B. Lee, J. Kim, K. Kang, *Mater. Res. Bull.* **2017**, *96*, 524; e) P. Byeon, H. B. Bae, H.-S. Chung, S.-G. Lee, J.-G. Kim, H. J. Lee, J. W. Choi, S.-Y. Chung, *Adv. Funct. Mater.* **2018**, *28*, 1804564; f) Y. Zhang, R. Zhang, Y. Huang, *Front. Chem.* **2019**, *7*, 335.

[28] a) K. A. Persson, B. Waldwick, P. Lazic, G. Ceder, *Phys. Rev. B* **2012**, *85*, 235438; b) A. K. Singh, L. Zhou, A. Shinde, S. K. Suram, J. H. Montoya, D. Winston, J. M. Gregoire, K. A. Persson, *Chem. Mater.* **2017**, *29*, 10159.

[29] E. W. Slessarev, Y. Lin, N. L. Bingham, J. E. Johnson, Y. Dai, J. P. Schimel, O. A. Chadwick, *Nature* **2016**, *540*, 567.
[30] R. E. Unger, K. Peters, A. Sartoris, C. Freese, C. J. Kirkpatrick, *Biomaterials* **2014**, *35*, 3180.
[31] X.-Y. Zhao, X.-F. Wang, L. Li, L. Zhang, D.-L. Shen, D.-H. Li, Q.-S. Jin, J.-Y. Zhang, *Diabetol. Metab. Syndr.* **2015**, *7*, 98.
[32] a) B. Scharf, C. C. Clement, V. Zolla, G. Perino, B. Yan, S. G. Elci, E. Purdue, S. Goldring, F. Macaluso, N. Cobelli, R. W. Vachet, L. Santambrogio, *Sci. Rep.* **2014**, *4*, 5729; b) Y.-F. Wang, H.-W. Shyu, Y.-C. Chang, W.-C. Tseng, Y.-L. Huang, K.-H. Lin, M.-C. Chou, H.-L. Liu, C.-Y. Chen, *Toxicol. Appl. Pharmacol.* **2012**, *259*, 177.
[33] J. Crossgrove, W. Zheng, *NMR Biomed.* **2004**, *17*, 544.
[34] M.-X. Zhao, Q. Xia, X.-D. Feng, X.-H. Zhu, Z.-W. Mao, L.-N. Ji, K. Wang, *Biomaterials* **2010**, *31*, 4401.
[35] I. Rajzer, E. Menaszek, L. Bacakova, M. Rom, M. Blazewicz, *J. Mater. Sci.: Mater. Med.* **2010**, *21*, 2611.
[36] R. Dugas, B. Zhang, P. Rozier, J. M. Tarascon, *J. Electrochem. Soc.* **2016**, *163*, A867.